Shakedown Analysis of Multi-layer Pavements Using Finite Elements and Linear Programming.

M.Z. Hossain
B.E., M.E.
Postgraduate Student, The University of Newcastle, NSW 2308, Australia

H.S. Yu
B.E., D.I.C., M.Sc., D.Phil
Senior Lecturer, The University of Newcastle, NSW 2308, Australia

Summary This paper presents a finite element formulation of the lower bound shakedown theorem to incorporate performance of pavement constituent materials into the pavement design. The formulation consists of a linear approximation of Mohr-Coulomb yield criterion and a statically admissible residual stress field. Shakedown limits are obtained from a total stress field that satisfies yield criterion everywhere in the region. A homogeneous isotropic half space is examined with different types of loading condition. An uniform load distribution produces higher shakedown limits than a trapezoidal load distribution. A significant difference between the shakedown limit and first yield load is obtained specially for high friction angles, which indicates as a reserve of strength within the domain beyond elastic limit. In the multi-layer pavement analysis, the influence of material stiffness and strength properties on the shakedown limit are examined for the trapezoidal load distribution case. Two distinct mechanisms towards failure are obtained in the shakedown analysis for different stiffness ratios among the layers.

1. INTRODUCTION

Direct calculations of exact shakedown load are difficult. Hence it is usual to adopt a device of calculating the best possible upper and lower bounds on the shakedown load. Sharp and Booker (1984) have suggested the possible use of shakedown theory in pavement design, which assume plane strain deformation across the travel direction and the wheel load being replaced by an infinitely long roller. In contrast, Collins and Cliff (1987) have adopted an alternative approach, which enables a full three dimensional upper bound analysis. This paper presents a lower bound shakedown formulation using a linear approximation of Mohr-Coulomb yield criterion. The residual stress field is modelled using 3-noded triangles where stress discontinuities are allowed to occur at the edges of each triangle. The lower bound shakedown limit is obtained from a total stress field that satisfies yield condition everywhere in the region. Application of the shakedown theorem is successfully examined using a half-space and a two-layer continuum of homogeneous soil. The variation of shakedown limits on different material and layer properties is illustrated which can be used to form the basis of design criteria.

2. LOWER BOUND SHAKEDOWN THEOREM

Melan's static shakedown theorem states that "If the combination of a time independent, self equilibrated residual stress field σ^r_{ij} and the elastic stresses σ^e_{ij} can be found which doesn't violate the yield condition anywhere in V and at anytime T, then the material will shakedown". Total stresses are then

$$\sigma_{ij} = \lambda\sigma^e_{ij} + \sigma^r_{ij} \tag{1}$$

where σ^r_{ij} are the residual stresses and λ is the shakedown factor. This lower bound shakedown factor λ lies between zero and actual shakedown factor λ_c. The determination of the best lower bound is considered as a problem of linear programming : the maximisation of the load multiplier λ, subject to the constraint that the yield condition is not violated.

2.1 Triangular Stress Element

The triangular element used to model the residual stress field under conditions of plane strain is shown in Figure 1. The variation of the residual stress throughout each element is assumed to be linear and each node is associated with three unknown stresses σ^r_x, σ^r_y, τ^r_{xy}. Each stress varies through an element according to

$$\sigma^r_x = \sum_{i=1}^{3} N_i\sigma^r_{xi} \; ; \; \sigma^r_y = \sum_{i=1}^{3} N_i\sigma^r_{yi} \; ; \; \tau^r_{xy} = \sum_{i=1}^{3} N_i\tau^r_{xyi} \tag{2}$$

Where σ^r_{xi}, σ^r_{yi} and τ^r_{xyi} are the nodal residual stresses and N_i are linear shape functions.
The shape functions are :

$$N_1 = (\xi_1 + \eta_1 + \zeta_1)\,/2A \;;$$
$$N_2 = (\xi_2 + \eta_2 + \zeta_2)\,/2A \;;$$

$$N_3 = (\xi_3 + \eta_3 + \zeta_3)\ /2A \quad (3)$$

where

$$\xi_1 = x_2y_3 - x_3y_2\ ;\ \eta_1 = y_2 - y_3\ ;\ \zeta_1 = x_3 - x_2$$
$$\xi_2 = x_3y_1 - x_1y_3\ ;\ \eta_2 = y_3 - y_1\ ;\ \zeta_2 = x_1 - x_3 \quad (4)$$
$$\xi_3 = x_1y_2 - x_2y_1\ ;\ \eta_3 = y_1 - y_2\ ;\ \zeta_3 = x_2 - x_1$$

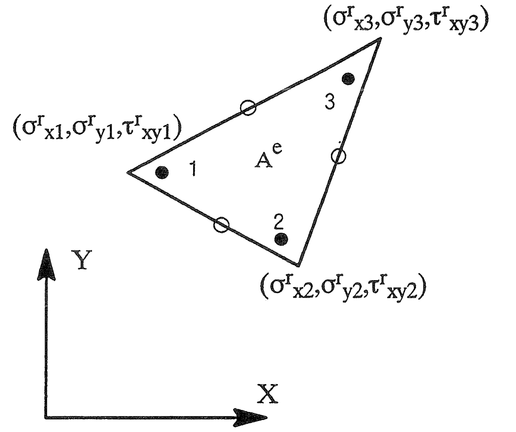

Figure 1. 3-Noded linear stress triangle

and $2A = |\ \eta_1\zeta_2 - \eta_2\zeta_1|$ is twice the element area. Statically admissible stress discontinuities are permitted at shared edges between adjacent triangles. If E denotes the number of triangles in the mesh, then there are $3E$ nodes and $9E$ unknown residual stresses.

2.2 Yield Criterion

Under the condition of plane strain, the Mohr-Coulomb yield criterion can be expressed as

$$F = (\sigma_x - \sigma_y)^2 + (2\tau_{xy})^2 - (2c\ \cos\phi - (\sigma_x + \sigma_y)\sin\phi)^2 \le 0 \quad (5)$$

Since we wish to formulate the lower bound theorem as a linear programming problem, the yield criterion is approximated as a linear function of the unknown stresses as presented by Sloan (1988). This linearized yield surface must lie inside the Mohr–Coulomb yield surface in stress space.

Letting

$$X = \sigma_x - \sigma_y\ ;\ Y = 2\tau_{xy}\ ;\ R = 2c\ \cos\phi - (\sigma_x + \sigma_y)\sin\phi \quad (6)$$

the Mohr–Coulomb yield criterion may be written as $X^2 + Y^2 = R^2$. In terms of the variables X and Y, this plots as a circle. And this surface can be approximated by an interior polygon with p sides and p vertices as shown in Figure 2. The X and Y coordinates of the kth and $(k+1)th$ vertices are given by

$$X_k = R\cos(\pi(2k-1)/p)\ ;\ Y_k = R\sin(\pi(2k-1)/p)$$
$$X_{k+1} = R\cos(\pi(2k+1)/p);\ Y_{k+1} = R\sin(\pi(2k+1)/p) \quad (7)$$

Each stress point with coordinates X and Y is located inside or on the yield polygon if

$$(X_{k+1} - X)(Y_k - Y) - (X_k - X)(Y_{k+1} - Y) \le 0;\ k = 1, 2, 3, \ldots p$$

Substituting equations (6) and (7) gives the linearized yield function as

$$A_k\sigma_x + B_k\sigma_y + C_k\tau_{xy} \le D\ ;\ k = 1, 2, 3\ \ldots\ldots p \quad (8)$$

in terms of residual stresses this equation becomes

$$A_k\sigma^r_x + B_k\sigma^r_y + C_k\tau^r_{xy} + \lambda(A_k\sigma^e_x + B_k\sigma^e_y + C_k\tau^e_{xy}) \le D \quad (9)$$

Where

$$A_k = \cos(2\pi k/p) + \sin\phi\cos(\pi/p)\ ;$$
$$B_k = \sin\phi\cos(\pi/p) - \cos(2\pi k/p)\ ;$$
$$C_k = 2\sin(2\pi k/p)\ ;$$
$$D = 2c\ \cos\phi\cos(\pi/p) \quad (10)$$

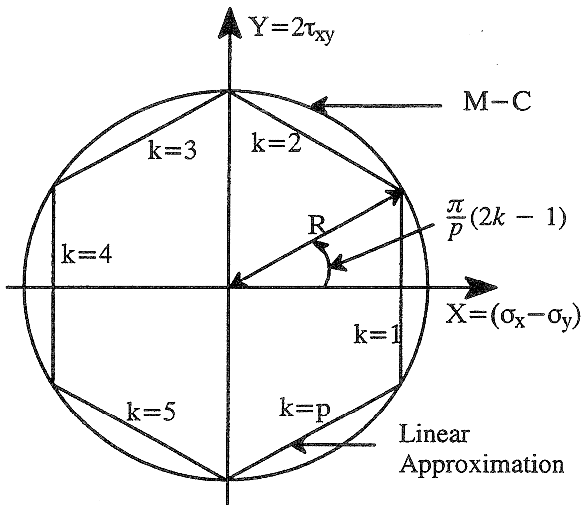

Figure 2. Linearized Mohr-Coulomb yield function (p=6)

This constraint is enforced at each nodal point for each element. The residual stress variation is assumed linear, but the elastic stresses are not necessarily linear. Hence, in order that equation (9) satisfies throughout the mesh it might be necessary to enforce this constraint at some other points in the triangle as well. In this study, the yield criterion is satisfied by both the residual stress and the total stress at six points for each triangle. Further increase in number of points does not change the result. Hence, six points for each triangle are considered enough for the mesh used in this study. Three of these points are at corner nodes and the rests are at middle points of the triangle arms.

(a1) Yield criterion at corner nodes by residual stresses

$$A_k\sigma^r_{xi} + B_k\sigma^r_{yi} + C_k\tau^r_{xyi} \le D \quad (11)$$

and by total stresses

$$A_k\ \sigma^r_{xi} + B_k\ \sigma^r_{yi} + C_k\ \tau^r_{xyi} + E_{ki}\ \lambda \le D \quad (12)$$

where

$$E_{ki} = A_k\ \sigma^e_{xi} + B_k\ \sigma^e_{yi} + C_k\ \tau^e_{xyi} \quad (13)$$

(a2) Yield criterion at middle of the arms by residual stresses

$$\frac{A_k}{2}\sigma^r_{xi} + \frac{A_k}{2}\sigma^r_{xj} + \frac{B_k}{2}\sigma^r_{yi} + \frac{B_k}{2}\sigma^r_{yj} + \frac{C_k}{2}\tau^r_{xyi} + \frac{C_k}{2}\tau^r_{xyj} \leq D \tag{14}$$

and by total stresses

$$\frac{A_k}{2}\sigma^r_{xi} + \frac{A_k}{2}\sigma^r_{xj} + \frac{B_k}{2}\sigma^r_{yi} + \frac{B_k}{2}\sigma^r_{yj} + \frac{C_k}{2}\tau^r_{xyi} + \frac{C_k}{2}\tau^r_{xyj} + E_{km}\,\lambda \leq D \tag{15}$$

where

$$E_{km} = A_k\sigma^e_{xm} + B_k\sigma^e_{ym} + C_k\tau^e_{xym} \tag{16}$$

and i,j are the two nodes of the triangle at the end of the concerned arm and m is the middle point of that arm.

The constraints imposed on the stresses at node i due to the linearized yield criterion may be summarised by the matrix equation

$$\left[A^i_{yield}\right]\left\{\sigma^{ri}\right\} = \left\{b^i_{yield}\right\} \tag{17}$$

where

$$\left[A^i_{yield}\right] = \begin{bmatrix} A_1 & B_1 & C_1 & \cdot & \cdot & E_{1i} \\ A_2 & B_2 & C_2 & \cdot & \cdot & E_{2i} \\ A_3 & B_3 & C_3 & \cdot & \cdot & E_{3i} \\ \cdot & \cdot & \cdot & \cdot & \cdot & \cdot \\ A_k & B_k & C_k & \cdot & \cdot & E_{ki} \\ \cdot & \cdot & \cdot & \cdot & \cdot & \cdot \\ A_p & B_p & C_p & \cdot & \cdot & E_{pi} \end{bmatrix} \tag{18}$$

$$\left\{\sigma^{ri}\right\}^T = \left\{\sigma^r_{xi}\ \sigma^r_{yi}\ \tau^r_{xyi}\ \cdot\ \cdot\ \lambda\right\} \tag{19}$$

$$\{b^i_{yield}\}^T = \{2c_i cos\phi cos(\pi/p), 2c_i cos\phi cos(\pi/p), \ldots, 2c_i cos\phi cos(\pi/p)\} \tag{20}$$

The coefficients A_k, B_k, C_k, D_k and E_{ki} are given by equations (10) to (16) and c_i is the cohesion at node i.

2.3 Objective Function

It is wished to find a set of residual stress distribution with a maximum possible factor, λ, which with elastic stresses will satisfy yield criterion all over the mesh. The problem can then be stated as

Minimise $\quad -\lambda$

Subject to $\quad [A_1]\{X\} = \{B_1\}$

$\qquad\qquad\quad [A_2]\{X\} \leq \{B_2\}$

Where

$$\{X\}^T = \{\sigma^r_{x1}, \sigma^r_{y1}, \tau^r_{xy1}, \sigma^r_{x2}, \sigma^r_{y2}, \ldots \sigma^r_{xN}, \sigma^r_{yN}, \tau^r_{xyN}, \lambda\}$$

$$[A_1] = \sum_{e=1}^{E}[A^e_{equil}] + \sum_{d=1}^{D}[A^d_{equil}] + \sum_{l=1}^{L}[A^l_{bound}]$$

$$[A_2] = \sum_{i=1}^{N}[A^i_{yield}]$$

$$\{B_1\} = \sum_{e=1}^{E}\{b^e_{equil}\} + \sum_{d=1}^{D}\{b^d_{equil}\} + \sum_{l=1}^{L}\{b^l_{bound}\}$$

$$\{B_2\} = \sum_{i=1}^{N}\{b^i_{yield}\}$$

Where $[A_1]$ is the matrix of equality constraints, $[A_2]$ is the matrix of yield constraints, $\{B_1\}$ and $\{B_2\}$ are the respective vectors containing strength properties. The coefficients are inserted into the appropriate rows and columns and N is the total number of nodes, E is the total number of elements, D is the total number of discontinuities and L is the total number of boundary edges.

3. APPLICATION OF SHAKEDOWN THEOREM

The finite element formulation of the lower bound shakedown theorem described in the previous section is applied to a half space and a two-layer continuum of homogeneous isotropic soil in this section.

3.1 Shakedown of Homogeneous Isotropic Half-Space under Moving Surface Loads

The mesh used to determine the shakedown limit of different soils is shown in Figure 3. It is anticipated that a horizontal loading will not produce symmetrical response into the soil. Hence, a full width of loading is considered in the computation. Stress boundary conditions are applied as shown in the Figure. Overall, the grids comprise 1296 nodes, 432 triangular elements and 615 stress discontinuities. The vertical extension of the domain is considered 200 times the half loaded width (B/2) and horizontal extension is 3B.

At first a homogeneous isotropic half space is examined. Moving load due to passage of a wheel is modelled (i) as Uniform load distribution and (ii) Trapezoidal load distribution. The uniform load distribution is considered for a plane which is across the travel direction, whereas the trapezoidal load distribution is for a plane which is along the travel direction. Assumption of a half space plane strain condition is more realistic for a plane which is across the travel direction. Hence, the uniform loading case satisfies the plane strain condition more accurately than the trapezoidal loading case. In the trapezoidal load distribution case, the wheel load is represented by an infinity wide roller as assumed in Sharp and Booker (1984). Figure 4 shows the idealised load distribution on the surface. Material characteristics are fixed by choosing cohesion (c) and angle of internal friction (ϕ). The Mohr-Coulomb yield circle is linearized by 48 sided regular polygon. The elastic stresses for the semi-infinite mass are computed using the analytical solution given by Poulos and Davis (1974). The problem is then to find the largest load factor λ for which the pavement will shakedown.

3.1.1 Shakedown limit for different friction angles (ϕ)

The influence of material friction angle (ϕ) on the shakedown limit is plotted in Figure 5. The shakedown limit increases significantly with the increase in friction angle, specially at high friction angle as shown in the Figure. The Figure also shows a comparison among the first yield load, the shakedown limit and the collapse load (Prandtl 1920) for a range of values of material friction angle. An increase in ϕ from 0 to 30 degrees produces about 300% of increase in the shakedown limit, which implies that the material friction angle affects the shakedown limit significantly. The Figure also indicates a significant difference between the shakedown limit and the first yield load, specially at high values of ϕ, indicating a reserve of strength within the domain.

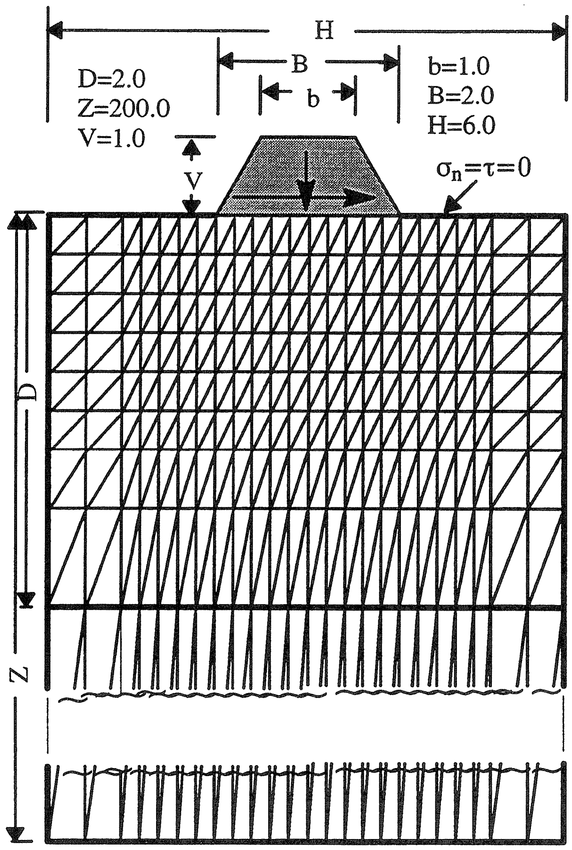

Number of nodes =1296
Number of independent coordinates = 250
Number of elements = 432
Number of discontinuities = 615

Figure 3. Mesh used in multi-layer analysis

3.1.2 Shakedown limit for different applied load distribution

A significant difference in the shakedown limit is found between the two cases of applied load distribution. In this study, three components of the residual stress σ^r_x, σ^r_y and τ^r_{xy} are taken into account in the uniform load distribution case whereas in the trapezoidal load distribution case only σ^r_x is present.

A higher shakedown limit is obtained in a two-dimensional analysis with the uniform load distribution than an one-dimensional analysis with the trapezoidal load distribution. Figure 6 compares the shakedown limit values obtained by various authors for different material friction angles. As described earlier, a significant difference in λ is obtained between the two-dimensional and the one-dimensional analyses. The shakedown limit obtained in this project using the one-dimensional analysis with the trapezoidal load distribution is in good agreement with the results reported by Sharp and Booker (1984). Idealisation of load distributions draws attention to have more realistic load-response mechanism. The one-dimensional analysis with the trapezoidal load distribution was supported by Sharp and Booker (1984) as a reasonable approach for pavement design. Hence, their approach is followed in this study to verify its performance.

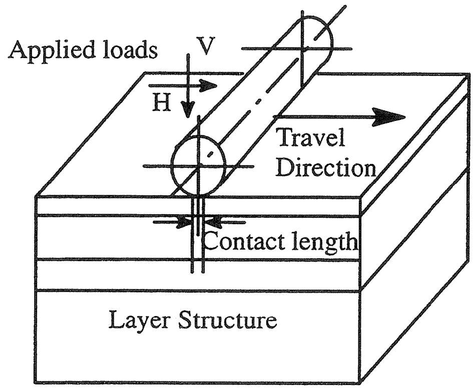

Figure 4a. Plane strain pavement and loading

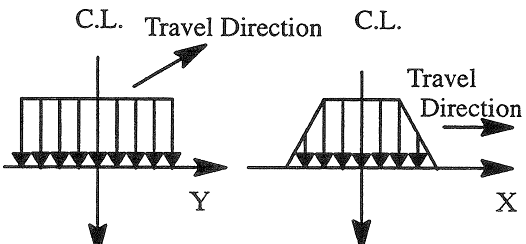

Figure 4b. Idealized load distribution

3.1.3 Effect of horizontal loading on shakedown load

The shakedown limit decreases dramatically with the increase in the surface frictional coefficient μ (ratio of horizontal load to vertical load) as shown in Figure 7. This means the horizontal force has a substantial influence on the shakedown limit through the elastic shear stress. The Figure also reveals two distinct patterns of shakedown limit variation. For sufficiently small values of μ, load is being carried to the sub-grade leading to a bearing type of failure, whereas for larger values of μ, load remains in the top layer leading to a shear type of failure. This shows good agreement with the finding of Sharp and Booker (1984).

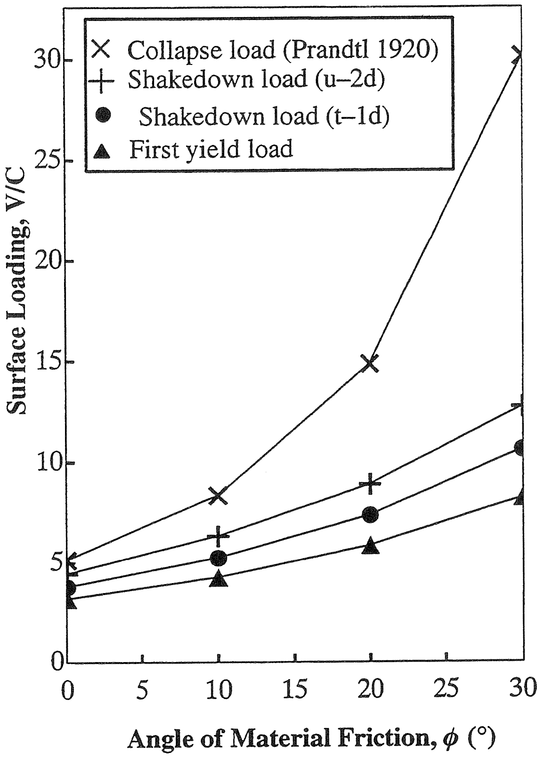

Figure 5. Influence of material friction angle on first yield, shakedown and collapse load

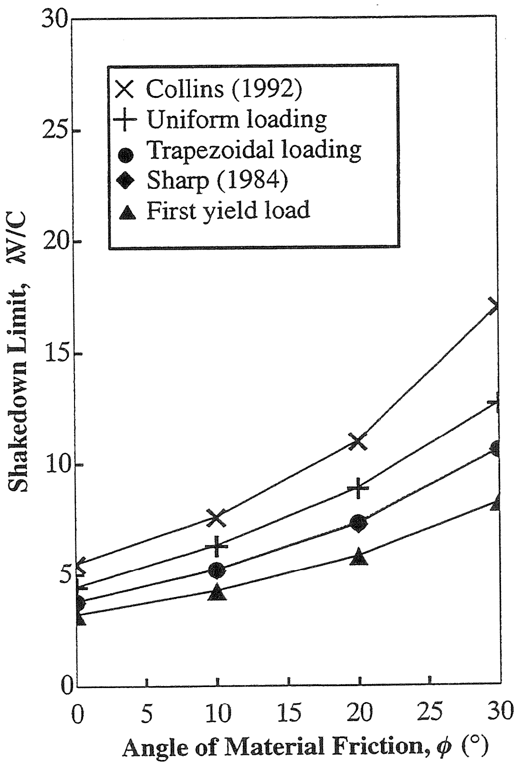

Figure 6. Comparison among Sharp(1984), Collins(1992) and this Project

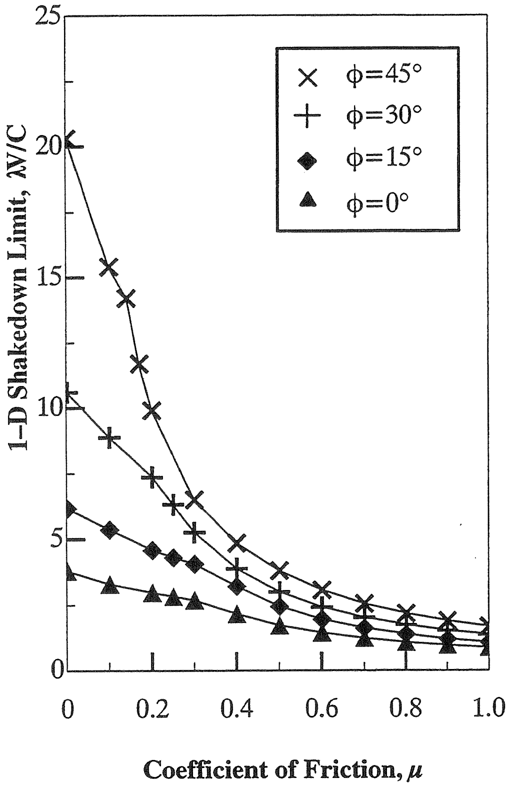

Figure 7. Influence of ϕ and μ on λ trapezoidal load distribution case

3.2 Shakedown of a Two-layer Half Space Under Moving Surface Load

Some aspects of a two-layer pavements are examined in this section. The elastic stresses for multi-layers are computed using Finite Layer Elastic Analysis (FLEA). It is assumed that material properties are homogeneous and isotropic in each layer. Parameters with *0* subscript represents the properties of lower layer. A number of studies have been performed with clay ($\phi=0°$). Although this idealisation differs from practical pavement, the tests are valuable as a qualitative indicator of performance and are readily extendable to frictional materials. Figure 8 shows the performance of a two-layer pavement subjected to normal wheel load only. Ratio of the surface layer stiffness to the sub-grade (lower layer) is varied with relative strength of the two layers being held constant. Again two distinct mechanisms of failure are obtained with the variation of E/E_0 as shown in the Figure. For higher values of E/E_0, stresses tend to remain in the surface layer. Residual stresses of tensile nature forms at the base of this layer, resulting a fatigue failure at this level. Significantly lower values of the shakedown limit are obtained in this study when compared with those reported by Sharp and Booker (1984) in this part of analysis. In their analysis, it seems that only total stresses satisfy the yield criterion. But the residual stresses, existed in the soil medium during the unloading should also not violate the yield criterion. Hence, the yield criterion needs to be satisfied by both the total and the residual stresses and this has been done successfully in this study. As a result, this study can be considered to produce a more accurate result than the model proposed by Sharp and Booker (1984). For lower values of E/E_0, more loads are distributed to the sub-grade, leaving a fatigue of compressive nature at the top of this layer. And it is clear that, there exists an optimum ratio of stiffness (E/E_0) at which the resistance to incremental collapse is maximum.

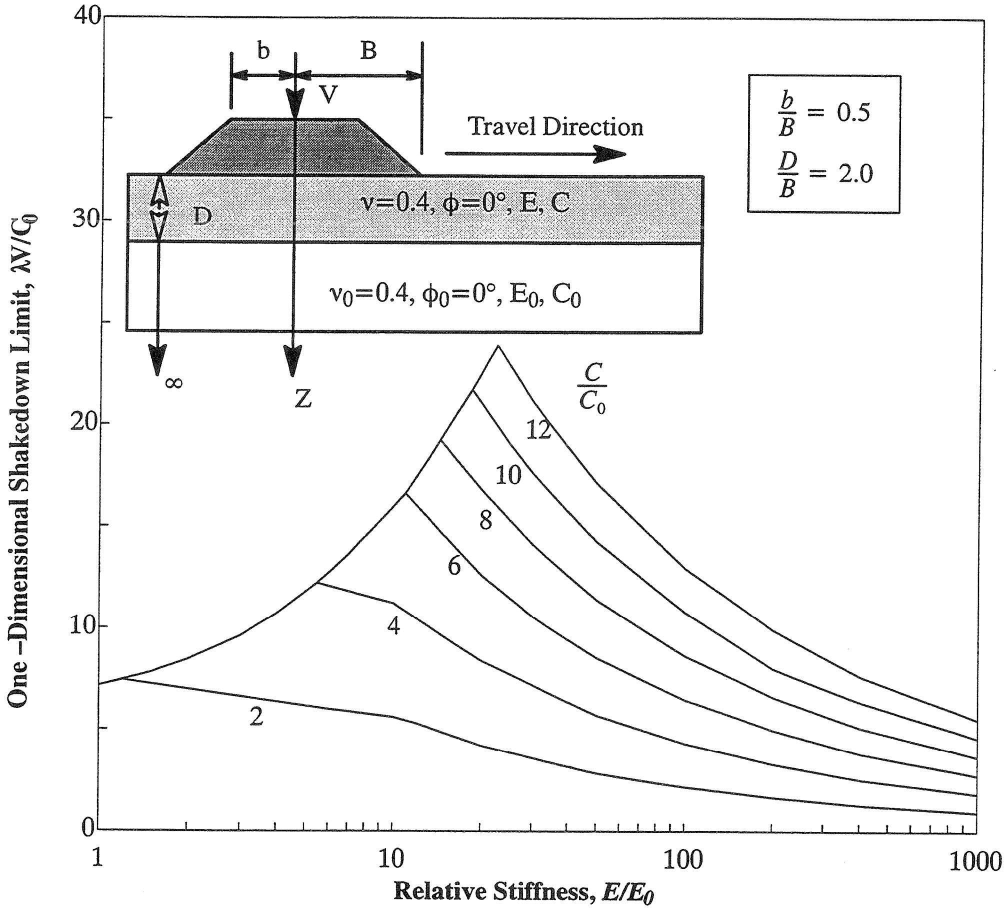

Figure 8. Influence of stiffness and strength on shakedown limit of a two-layer system

4. CONCLUSIONS AND RECOMMENDATIONS

The lower bound shakedown theorem produces a shakedown limit well below the collapse load, specially by one-dimensional analysis. The approximation of roller type of loading in the one-dimensional analysis is likely to overestimate the stresses in the regions other than the vertical plane through the centre line. The two-dimensional analysis with a uniform loading produces a higher shakedown limit than the one-dimensional analysis with a trapezoidal loading, partly because of the addition of more components of residual stress. Hence more investigation, specially of an experimental nature is needed to verify the model performance. The influence of layer thickness on the shakedown limit will be investigated also for cohesive-frictional materials. An upper bound shakedown analysis will need to be carried out in order to find the actual range of shakedown load.

5. ACKNOWLEDGMENTS

The authors would like to express their sincere gratitude to A/Prof S.W. Sloan for many useful discussions. Thanks also goes to A/Prof J.C. Small for his assistance in allowing us to use FLEA program.

6. REFERENCES

Poulos, H.G. and Davis, E.H. (1974). *Elastic Solutions for Soil and Rock Mechanics*, Wiley, Sydney.

Collins, I.F. and Cliffe, P.F. (1987). Shakedown in Frictional Materials Under Moving Surface Loads, *Int. J. for Numerical and Analytical Methods in Geomechanics*, Vol 11, pp. 409–420.

Collins, I.F.; Wang, A.P. and Saunders, L.R. (1993). Shakedown Theory and the Design of Unbound Pavements, *Road and Transport Research*, Vol 2, No.4, pp. 28–39.

Sharp, R.W. and Booker, J.R. (1984). Shakedown of Pavements under Moving Surface Loads, *Journal of Transportation Engineering*, Vol 110, pp. 1–14.

Sloan, S.W. (1988). Lower Bound Limit Analysis using Finite Elements and Linear Programming, *Int. J. of Numerical and Analytical Methods in Geomechanics*, Vol 12, pp. 61–77.